TRANSIENT ANALYSIS OF THE WOLSONG UNITS 2/3/4 MODERATOR FOR 35% RIH BREAK WITH LOSS OF ECC INJECTION USING CFX-4.4

CHURL YOON, BO WOOK RHEE, BYUNG-JOO MIN

Korea Atomic Energy Research Institute
150 Dukjin-Dong, Yusong-Gu
Daejeon 305-353, Korea
ex-cy@kaeri.re.kr; bwrhee@kaeri.re.kr; bjmin@kaeri.re.kr

ABSTRACT

A 3-D CFD model was developed for the transient simulation of the moderator circulation inside the Calandria vessel, using a commercial code CFX-4.4. For the initial condition, a steady-state moderator circulation was analyzed for 103% full power (Yoon et al., 2002). The transient moderator analysis was performed for the 35% RIH(Reactor Inlet Header) break with loss of ECC(Emergency Core Cooling) injection. Until 40 sec after LOCA, local subcooling in the core region was bounded well over the minimum subcooling of 30°C. For local subcooling below 30 °C, film boiling can occur in certain conditions.

1. INTRODUCTION

The Calandria tube contains a co-axial pressure tube, in which fuel bundles are located and the D_2O coolant fluids flow. For some loss of coolant accidents with a coincidental loss of emergency core cooling in a CANDU reactor, the temperature of the pressure tubes could increase and the pressure tube could strain (i.e., balloon) to contact its surrounding Calandria tube(PT/CT contact). Following the PT/CT contact, there is a spike in the heat flux to the moderator surrounding the Calandria tube, which leads to sustained CT dryout. The prevention of CT dryout following PT/CT contact depends on available local moderator subcooling. Higher moderator temperatures (lower subcooling) would decrease the margin of the Calandria tubes to dryout in the event of PT/CT contact. Therefore it is one of the CANDU safety issues to estimate the local moderator subcooling capability for LOCA transients. The objectives of this study are to develop a 3-D CFD model for predicting the temperature distributions of the moderator inside the Calandria vessel by using a commercial code, CFX-4.4 (AEA Technology), and to analyze the moderator transient for LLOCA with LOECC by implementing local heat load data from single channel analyses using CATHENA and CHAN codes.

2. CFD MODEL FOR PREDICTING THE CANDU MODERATOR TEMPERATURE

The reactor vessel of the CANDU-6 NPPs (Nuclear Power Plants) is an intended cylindrical tank (called 'Calandria') filled with moderator, which is 6 meters long with a diameter of 7.6 meters. The large cylindrical tank has eight inlet nozzles and two outlet ports, which are connected to two combined cooling loops. Inside the Calandria shell, there is a co-axial cylindrical core region with a smaller diameter. In the core region, a matrix of 380 pipes are located. The four inlet nozzles are located at the middle of each left and right sidewall, pointing upward. On the bottom of the large cylindrical tank, two outlet ports are located asymmetrically. Removing all the control mechanisms and monitoring devices, the simplified geometry for the moderator CFD analysis is shown in Fig. 1. Two closely located inlet nozzles are combined into a rectangular block. The standard k-ε turbulence model associated with logarithmic wall treatment is used to model turbulence generation and dissipation within the vessel. Buoyancy forces are modeled using the Boussinesq approximation in which the density is assumed to be a linear function of temperature.

The matrix of the Calandria tubes in the core region is simplified by the porous media approach (Todreas and Kazimi, 1990). The hydraulic resistance experienced by fluid flowing through the core region is accounted for as source terms of the momentum equations. The hydraulic resistance consists of two factors; form drag and friction drag. Neglecting the fact that hydraulic resistance is dependent on the attack angle between the flow direction and tube axis, the moderator fluid flow is conveniently decomposed into axial flow and lateral flow. For axial flow, there is no form drag. Thus, once we assume that we can decompose fluid flow into x, y, and z components, the hydraulic resistance of the axial flow could be expressed by the conventional correlations of frictional pressure loss in a cylindrical pipe. For the transverse (lateral) flow across the tube bank, Hadaller et al. (1996) investigated the pressure drop of fluid flows crossing staggered and in-line tube banks, in which the Reynolds number range is 2,000 to 9,000 and pitch to tube diameter ratio is 2.16. The obtained empirical correlation for the pressure loss coefficient(PLC) is expressed as

$$PLC \equiv \frac{\Delta P}{N_r \cdot \rho \cdot \frac{V_m^2}{2}} = 4.54 * Re^{-0.172}, \qquad (1)$$

where P = pressure (N/m^2),
N_r = number of rows, and
V_m = velocity before obstruction.
The implementation procedure follows the previous publication (Yoon et al., 2002).

3. TRANSIENT HEAT LOAD FOR 35% RIH WITH LOECC

The transient condition starts after the reactor inlet header break. The starting condition for the transient analysis is the steady-state solution. From the Large LOCA analysis, CATHENA predictions (0 to 40 s) and CHAN predictions (after 40 s) gave the results that some of the pressure tubes in the critical pass (i.e. downstream of the break) contact with the Calandria tubes from 20 to 40 seconds, and then are followed by the rest of the pressure tubes in the broken loop between 40 and 2000 seconds. Note that the Class IV power is available for this analysis. The moderator analysis for LLOCA/LOECC without Class IV power will be performed in future researches.

The heat sources of the moderator during this transient are divided into the heat load due to fission product decay and neutronic power, and the heat load due to PT/CT contact. The transient consists of a Blowdown Phase (0 to 40 sec) and a Post-Blowdown Phase (after 40 sec). Fig. 2 shows the total heat load to moderator and the power to the heat exchangers for a 35% RIH with Loss of ECC injection. The moderator heat load curve has three distinct humps, which are due to the LOCA power pulse at around 1 sec, the number of PT/CT contacts in the critical pass at 20~40 sec, and the contacts of the rest of the pressure tubes in the broken loop after 40 sec. For the case of Class IV power available, the heat removed by the heat exchangers exceeds the heat input shortly after reactor trip. It leads to a continuous decrease in the average moderator temperature.

3.1 Heat Load to Moderator under Normal Operating Conditions

For the 2064MW(th) nuclear reactor, the nuclear energy deposited in the moderator from gammas and neutrons is 78.7 MW and the total energy deposition in the reflector is 5.9 MW at full power. Among the total heat load of 96.7 MW to moderator, only 4.3 MW is transferred through the Calandria tube surfaces. Table 1 summarizes the moderator system heat load during steady-state operations at full power, calculated from the physical studies by using the ANISN code (Kim et al., 1995). Under normal operating conditions, direct heating of gammas and neutrons generates most heat load to the moderator, and the heat to the moderator by heat conduction and convection is a small portion of the total heat load.

For conservative analysis, the total heat load to the moderator is taken to be 103 MW(103%) consisting of 96.7 MW to the core and 6.3 MW to the reflector region. The spatial heat distribution of the core region is calculated based on the actual power map. The power distribution in the reflector region was assumed uniform for simplicity, and was maintained at 6.1% of the total heat load to the moderator due to fission product decay and neutronic power.

3.2 Blowdown Phase (0 ~ 40 sec)

Reactor trip occurs at about 0.43 seconds. Leakage of primary coolant during LOCA induces the power pulse due to neutronic power, which gives a sharp peak of the heat load to the moderator at about 1 sec. The heat load to the moderator due to fission product decay decreases continuously all over the transient. After 20 sec, the total heat load to moderator consists of heat from direct heating ("B" in Fig. 2) and the heat from PT/CT contact ("A" in Fig. 2). The heat load distribution from direct heating is assumed to follow the power distribution of normal operating conditions, while the heat from PT/CT contacts is exerted on the local areas at specific locations.

All the channels of the critical core pass (95 channels) of the broken loop are divided into six groups based on average power. It is assumed that the broken loop is located in the hotter side ("B" side in Fig. 1). The heat loads due to PT/CT contact for one representative channel of the first four groups are obtained by CATHENA analysis, at every time step. For this six-group method, it is observed in the CATHENA analysis that the representative channels of the last two groups with lower power levels (group 5 & group 6) have no PT/CT contact during the blowdown phase. For each group, only one channel generating the highest power was analyzed by CATHENA for conservatism. Each peak in the second hump in Fig. 2 represents the heat spike of different channels at different bundle locations due to PT/CT contacts, caused by ballooning and sagging.

3.3 Post-Blowdown Phase (After 40 sec)

In the post-blowdown phase, the PT/CT contact takes place in each of the 190 channels of the broken loop (critical core pass as well as non-critical core pass). The channels of the non-critical core pass are also divided into six groups in such a way that the channels of each of these groups are the neighboring channels of the same group of the critical core pass. The heat load through PT/CT contact for each of the bundles of one representative channel of each of the groups of the critical core pass as well as the channels of the non-critical core pass are calculated by the CHAN code. Since the steam flow of 10 g/s generates more heat than 8 g/s or 5 g/s due to PT/CT contact up to 500 seconds, the analysis is performed for the 10 g/s steam flow.

4. SIMULATION RESULTS

The steady state computation using CFX-4.4 was performed in an HP-C3600 workstation. The convergence criteria were the enthalpy residual reduction factor of 10^{-3} and the largest mass residual of 10^{-6}. Because the energy equation and momentum equations are strongly interrelated in this computation, the algebraic multi-grid solver and false time stepping technique were adapted to accelerate the converging speed for the energy equation. The number of steady computation iterations was about 200,000~300,000. The transient computation was performed in the same machine starting from the steady-state results, with time steps of 0.05 sec or 0.1 sec. For each time step, more than 100 iterations were required to reach the enthalpy residual reduction factor of 10^{-3} and the mass residual of 10^{-5}.

The velocity fields and temperature distributions at the initial condition and every 10 sec after LOCA are presented in Figs 3 to 6. The results of the three cross-sectional planes orthogonal to the z-axis are plotted in one figure. The three cross-sectional planes include two planes, (a) & (c), cutting across one outlet and two inlet nozzles, and one middle plane, (b), containing neither an inlet nozzle nor an outlet. The results of the side views from the "B" side, (d), are also presented.

4.1 Steady-State Result for a Operating Condition

Under normal operating conditions, the calculated maximum temperature of the moderator is 82.9 °C at the upper center region of the core, which corresponds to the minimum subcooling of 24.8 °C. In Figs. 3(a) and 3(c), flow reversal is observed only for the injected fluid from the inlet nozzle far from the outlet port. The two injected fluids meet together at an angle of about 50° over the horizontal centerline, where the jet reversal occurs. The reversed fluid goes down to the bottom, guided by the circumferential lower vessel wall. This asymmetry of flow pattern is induced by the interaction between the buoyancy forces and the inlet jet momentum forces. The velocity vectors in the core region are relatively small compared to those of the reflector region due to hydraulic resistance in the core region. In Figures 3(a) and 3(c), the temperature distribution shows a steep change of temperature around the jet reversal area. In this area, the fluid from the opposite side nozzle heated during travel suppresses the cold injected fluid. The hottest spot is located at the upper center area of the core region, which slightly tilts to one side from the vertical centerline.

4.2 Blowdown Phase (0 ~ 40 sec)

The heat load involved in this phase consists of two parts; one is the exponentially decreasing direct heating by the gamma-ray from fission products, and the other is the convective heat transfer from PT/CT contact in the critical path. While the spatial distribution of direct heating follows the operating power distribution, the contact heat transfer occurs at a specific location according to the results of the CATHENA analysis. For the time period of 0 ~ 20 sec after LOCA, PT/CT contact does not occur and the special shape of the heat load to the moderator is the same as that of the normal operating conditions. Figure 4 shows the predicted moderator circulation at 20 sec after LOCA. Because the power is continuously decreasing except the sharp power pulse at 1 sec, the overall moderator temperature is lower than normal operating conditions.

Figure 5 & 6 present the moderator circulation and temperature distribution at 30 sec and 40 sec after LOCA, respectively. Due to PT/CT contacts, the flow pattern and the temperature distribution during this period (20 ~ 40 sec after the break) experience some local changes. For the "D" side (Fig. 1) of the core region, the heat load to the moderator by direct heating decreases down to one fifth of the power level of the normal operating conditions. On the "B" side (Fig. 1) of the core region, localized high heat loads by PT/CT contacts appear at certain locations. Due to the lower buoyancy forces in the "D" side of the core region, the reversed injected fluids penetrate more deeply inside the core region in (a) and (c) of Figs. 5 & 6. Localized high temperature contours appear at the location of the second to the fourth fuel bundle (counted from "C") of the first group channels (O17 and N16) in (c) and (d) of Figs. 5 & 6.

The minimum subcooling over the full domain inside the Calandria vessel and the local subcooling at the location of the N16 channel are displayed along with the transient time in Fig. 7. The minimum subcooling occurs at the upper corners of the Calandria subshell. The saturation temperature at this location is hydro-statically calculated to be 107.67°C, when the cover gas pressure is 18.0 kPa(g) and density of the moderator is 1084.7 kg/m^3. Similarly, the saturation temperature at the N16 location is 115.02°C. Because of the lower saturation temperature at the upper corners of the subshells, the minimum subcooling over the domain occurs at the subshells even though the highest temperature sometimes appears in the core region during the transient. The minimum subcooling increases continuously due to the descrending total heat load to the moderator during the transient. The solid line in Fig. 7 is local subcooling of the N16 channel surface, where the highest bundle temperature appears. The power pulse at around 1 sec induces instant decrease of the N16 local subcooling. The N16 local subcooling increases gradually after 3 sec until 20 sec, when the local subcooling of the N16 channel goes down due to PT/CT contact. Consequently, local subcooling in the core region is bounded well over the minimum subcooling of 30°C. For local subcooling below 30 °C, film boiling can occur in certain conditions.

4.3 Post-Blowdown Phase

The calculation of post-blowdown phase has not been finished yet, so the results are not presented in this paper. Further computation over 40 sec after the LOCA is in progress.

5. CONCLUSIONS

In this study, a new 3-D CFD analysis technique to predict CANDU-6 moderator circulations for 35% RIH breaks with loss of ECC injection was developed by implementing the localized transient heat load to the moderator. The transient heat load to moderator was obtained from the single channel analysis by the CATHENA and CHAN codes. The heat loads were implemented as source terms of the energy equation into the cells at the locations of each channel and bundle. The calculation has been successfully done until the end of the blowdown phase.

The observations are as follows: The effect of power pulse around at time = 1 sec is negligibly small because the total mass of the moderator is relatively large compared to the work of this pulse. Until 20 sec, the heat load to moderator is continuously decreasing except the sharp power pulse at 1 sec, so that the overall moderator temperature decreases. Due to the lower buoyancy forces in the "D" side of the core region, the reversed injected fluids penetrate more deeply inside the core region. Due to the PT/CT contacts (20 ~ 40 sec), localized high temperature contours appear at the location of the second to the fourth fuel bundle (counted from "C") of the first group channels (O17 and N16). During the transient until 40 sec after LOCA, local subcooling in the core region is bounded well over the minimum subcooling of 30°C. For local subcooling below 30 °C, film boiling can occur in certain conditions.

The further computation over 40 sec after the LOCA will be studied in the future.

ACKNOWLEDGEMENT

This study has been carried out as a part of the Development of Safety Issue Relevant Assessment System and Technology for CANDU NPPs program supported by Korea Ministry of Science & Technology.

REFERENCES

1. L.N. Carlucci and I. Cheung, The Effects of Symmetric/Asymmetric Boundary Conditions on the Flow of an Internally Heated Fluid, *Numerical Methods for Partial Differential Equations*, **2**, pp 47-61 (1986).

2. W.M. Collins, PHOENICS2 Model Report for Wolsong 2/3/4 Moderator Circulation Analysis, 86-03500-AR-053, (1995).
3. G.I. Hadaller, R.A. Fortman, J. Szymanski, W.I. Midvidy and D.J. Train, Fricktional Pressure Drop for Staggered and In Line Tube Bank with Large Pitch to Diameter Ratio, *Preceedings of 17th CNS Conference*, Federiction, New Brunswick, Canada (1996).
4. Y.I. Kim and K.Y. Kim, Radiation Heating Report, Rev. 2, 86-03320-AR-004, (1995).
5. P. Soedijono, W.M. Collins, and T. De, Moderator Analysis for In-Core and Out-of-Core Loss of Coolant Accident (LOCA), 86-03500-AR-052, (1995).
6. N.E. Todreas and M.S. Kazimi, *Nuclear System II: Elements of Thermal Hydraulic Design*, Chap. 5, Hemisphere Publishing Corporation (1990).
7. C. Yoon, B.W. Rhee, and B.-J. Min, Steady State 3-D Simulation of CANDU6 Moderator Circulation Under the Normal Operating Condition, *Canadian Nuclear Society 22nd Nuclear Simulation Symposium*, Ottawa, Ontario, Nov. 3-5 (2002).

Table 1. Moderator system heat load during steady state operations at full power (from ref. 4)

COMPONENT	HEAT LOAD (MW)
Heat generated in	
a) Moderator	78.7
b) Reflector	5.9
c) Calandria Tubes	4.3
d) Guide Tubes and Reactivity Mechanisms	2.7
Heat transfer from	
a) Calandria Shell and Tubesheets	1.7
b) Fuel Channels	3.0
Heat loss from	
a) Moderator pipings	- 0.3*
Heat gain from	
a) Moderator pumps	0.7
TOTAL	96.7 MW_{th}

* Negative sign indicates heat loss.

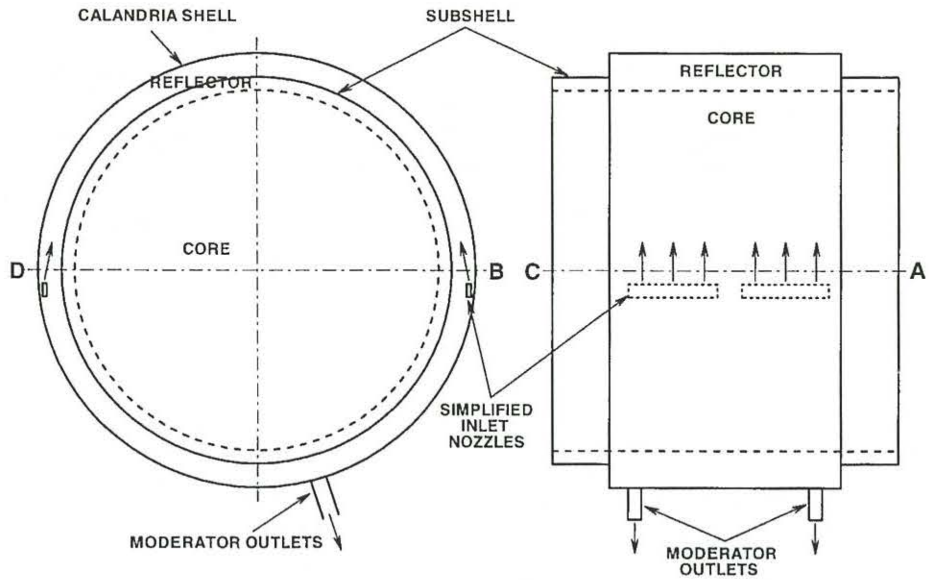

Figure 1. Simplified geometry of Wolsong 2/3/4 Calandria vessel

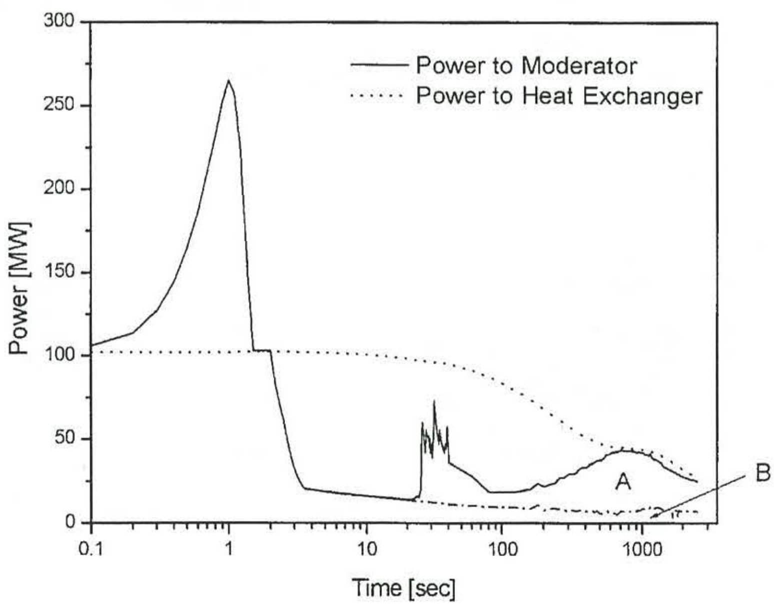

Figure 2. Total power to moderator and power to heat exchanger for 35% RIH with Loss of ECC injection

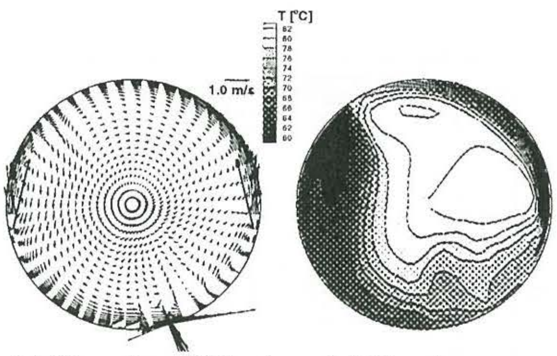

(a) View from "C", at z = 1.418 meter

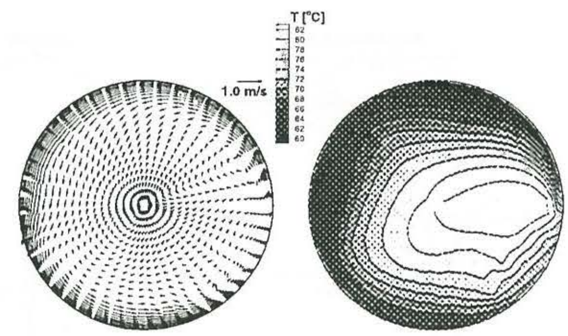

(b) View from "C", at z = 3.0 meter

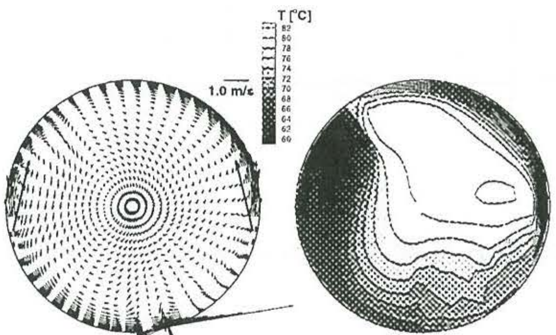

(c) View from "C", at z = 4.582 meter

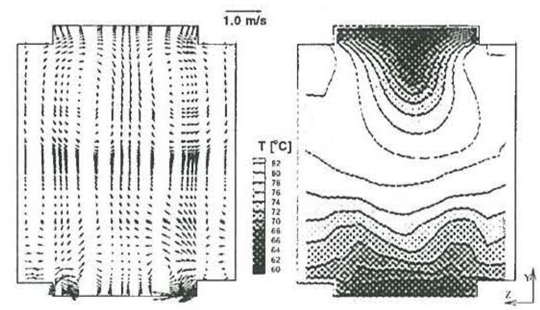

(d) View from "B", at x = 0.3 meter

Figure 3. Velocity fields and temperature distributions of CANDU-6 moderator under normal operating condition

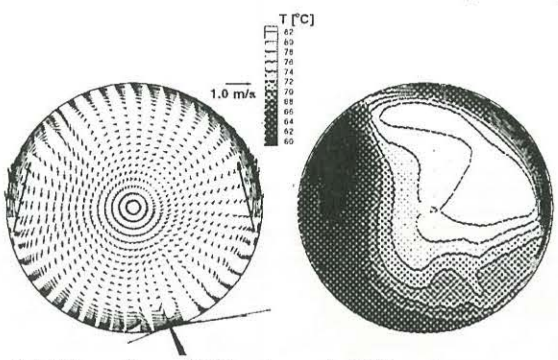

(a) View from "C", at z = 1.418 meter

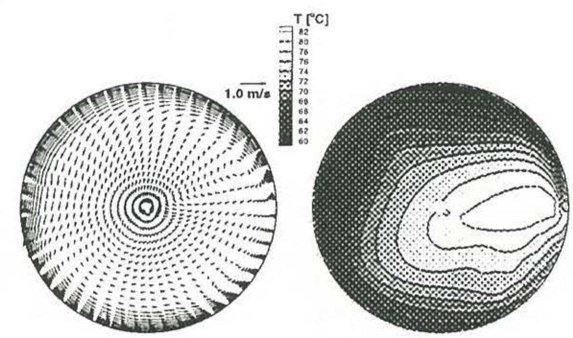

(b) View from "C", at z = 3.0 meter

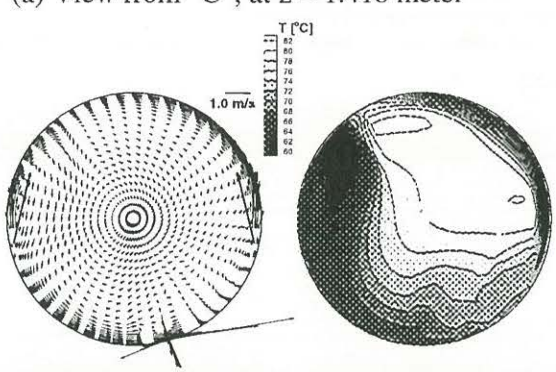

(c) View from "C", at z = 4.582 meter

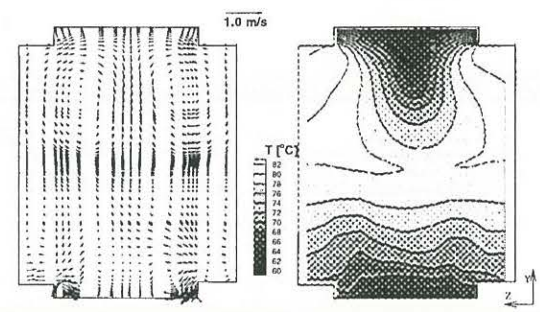

(d) View from "B", at x = 0.3 meter

Figure 4. Velocity fields and temperature distributions of CANDU-6 moderator at 20 sec after LOCA

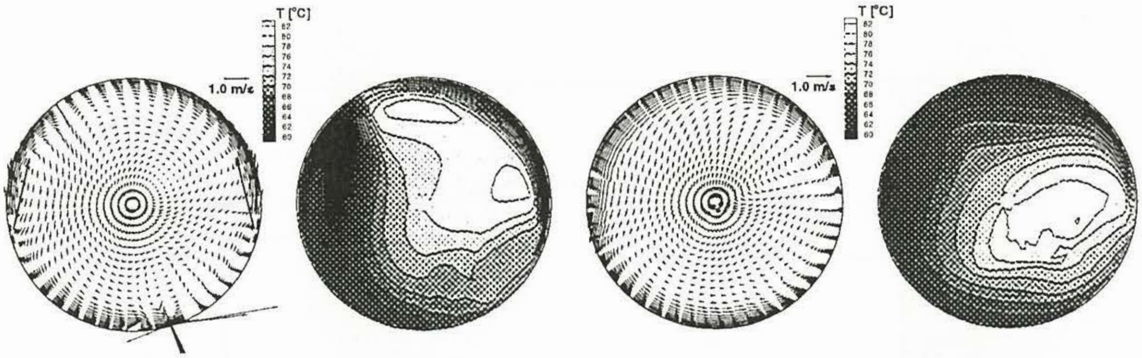

(a) View from "C", at z = 1.418 meter (b) View from "C", at z = 3.0 meter

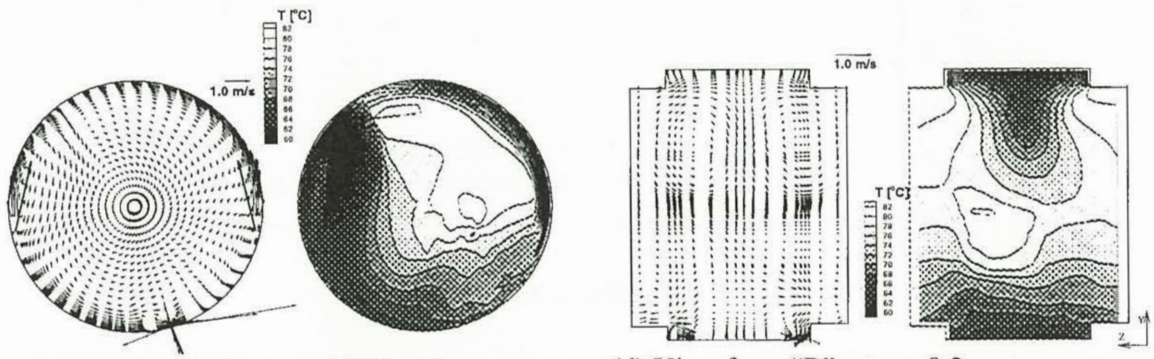

(c) View from "C", at z = 4.582 meter (d) View from "B", at x = 0.3 meter

Figure 5. Velocity fields and temperature distributions of CANDU-6 moderator at 30 sec after LOCA

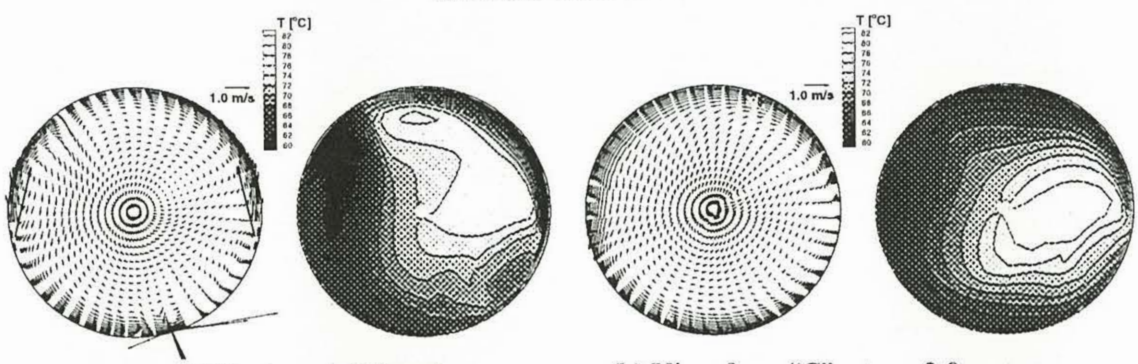

(a) View from "C", at z = 1.418 meter (b) View from "C", at z = 3.0 meter

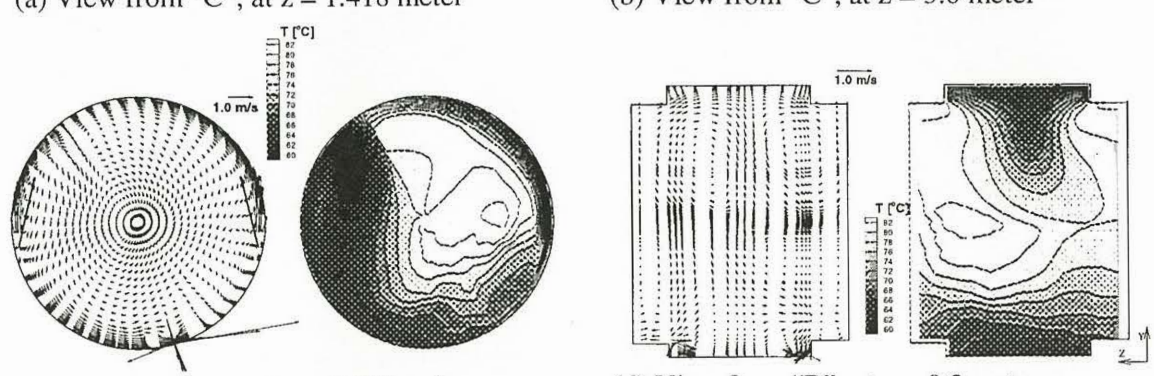

(c) View from "C", at z = 4.582 meter (d) View from "B", at x = 0.3 meter

Figure 6. Velocity fields and temperature distributions of CANDU-6 moderator at 40 sec after LOCA

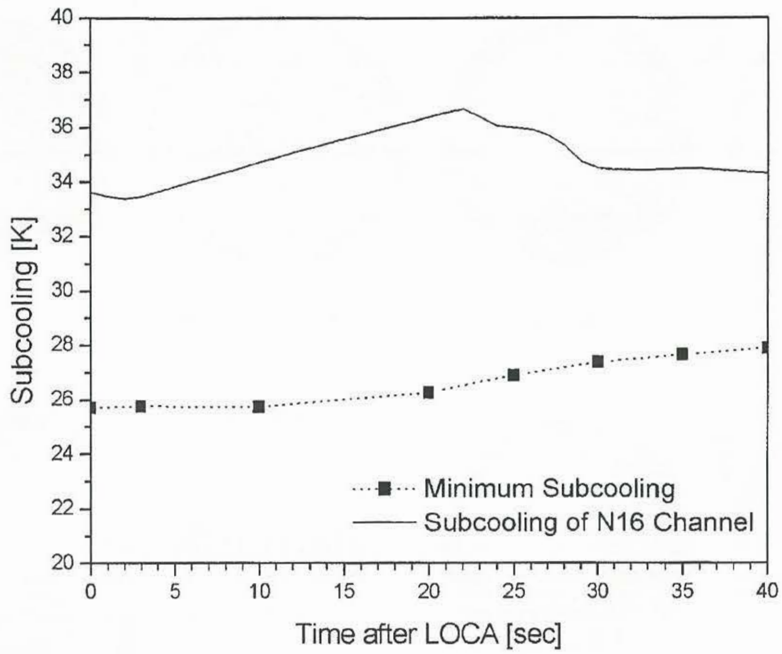

Figure 7. Minimum subcooling of moderator and local subcooling at the location of N16 channel